Hindawi
International Journal of RF and Microwave Computer-Aided Engineering
Volume 2023, Article ID 2232674, 11 pages
https://doi.org/10.1155/2023/2232674

Research Article

Dual-Band Metamaterial-Based EBG Antenna for Wearable Wireless Devices

Trong Hieu Dam,[1] Minh Thuy Le,[1] Quoc Cuong Nguyen,[1] and Thanh Tung Nguyen[2]

[1]*School of Electrical and Electronic Engineering, Hanoi University of Science and Technology, Hanoi, Vietnam*
[2]*Institute of Materials Science, Vietnam Academy of Science and Technology, Hanoi, Vietnam*

Correspondence should be addressed to Minh Thuy Le; thuy.leminh@hust.edu.vn

Received 22 April 2023; Revised 9 May 2023; Accepted 13 May 2023; Published 2 June 2023

Academic Editor: Xiao Ding

In this paper, a wearable dual-band T-shaped antenna using a coplanar waveguide (CPW) fed operating at 2.4 GHz and 5.2 GHz bands is proposed for onbody wireless communications applications. Without the metamaterial-based electromagnetic bandgap (EBG) layer, the original antenna covers two bands from 1.96 GHz to 2.77 GHz and from 5.07 GHz to 5.35 GHz. The antenna efficiency decreases when it is placed on the human arm due to the interference from the human body to the antenna, as shown by a high specific absorption rate (SAR) value. These SAR values are reduced to 77.1% at 2.4 GHz and 91.7% at 5.2 GHz by the proposed EBG. The antenna gain is therefore improved to 1.4 dBi at 2.4 GHz and 6.25 dBi at 5.2 GHz. The antenna prototype is evaluated using a Wi-Fi wearable device, resulting in an improved signal-to-noise ratio (SNR) of 6-12 dB.

1. Introduction

Nowadays, with the increase in average age in developed and developing countries, a telehealth monitoring system is a promising healthcare solution that allows elderly people to live alone. In this kind of system, wearable wireless devices are required to measure and collect human health parameters. Among them, the wearable antenna is an essential part of deciding the wireless communication quality [1–5]. The desired wearable antenna operates well when placed on the human body. In addition, it is compact and integrated into sensing circuits with a stable performance. To satisfy the IEEE 802.15 or IEEE 802.11 wireless local area network physical layer standards for most telemonitoring systems, a dual-band antenna at 2.4 GHz and 5.2 GHz bands design must be developed. However, the antenna performance is strongly affected by interference from the human body. To maintain its performance at both operation bands, several broadband and multiband antennas have been proposed based on the dipole, monopole, and slot antennas in [6–8]. It is indeed worth noting that while some flexible antennas were introduced in [9–11], they were not specifically designed for wearable devices. Regarding the size limitations of wearable devices, we have taken into consideration previous studies such as [12–14]. In [12–14], planar inverted-F antennas were utilized; however, their dimensions were relatively large ($0.68\lambda \times 0.52\lambda$ in [13] and $0.67\lambda \times 0.55\lambda \times 0.06\lambda$ in [14]), rendering them incompatible with wearable devices. Additionally, a dual-band monopole antenna was presented in [15], but it exhibited a narrow bandwidth of only 5.7% and 3.78% at 2.45 GHz and 5.85 GHz, respectively. As we mentioned before, unlike traditional antennas, which are generally positioned in free space, wearable antennas are located near human tissues. These tissues have a high dielectric constant, affecting the antenna performance such as reflection coefficient (S_{11}), bandwidth, gain, and radiation characteristics [15]. Furthermore, electromagnetic wave radiated from a wearable antenna is regulated not to be unsafe for human tissue health [16]. It is qualified by a specific absorption rate (SAR) level. In general, a maximum SAR value of 2 W/kg averaged over every 10 grams of tissue is required and set by the International Commission on

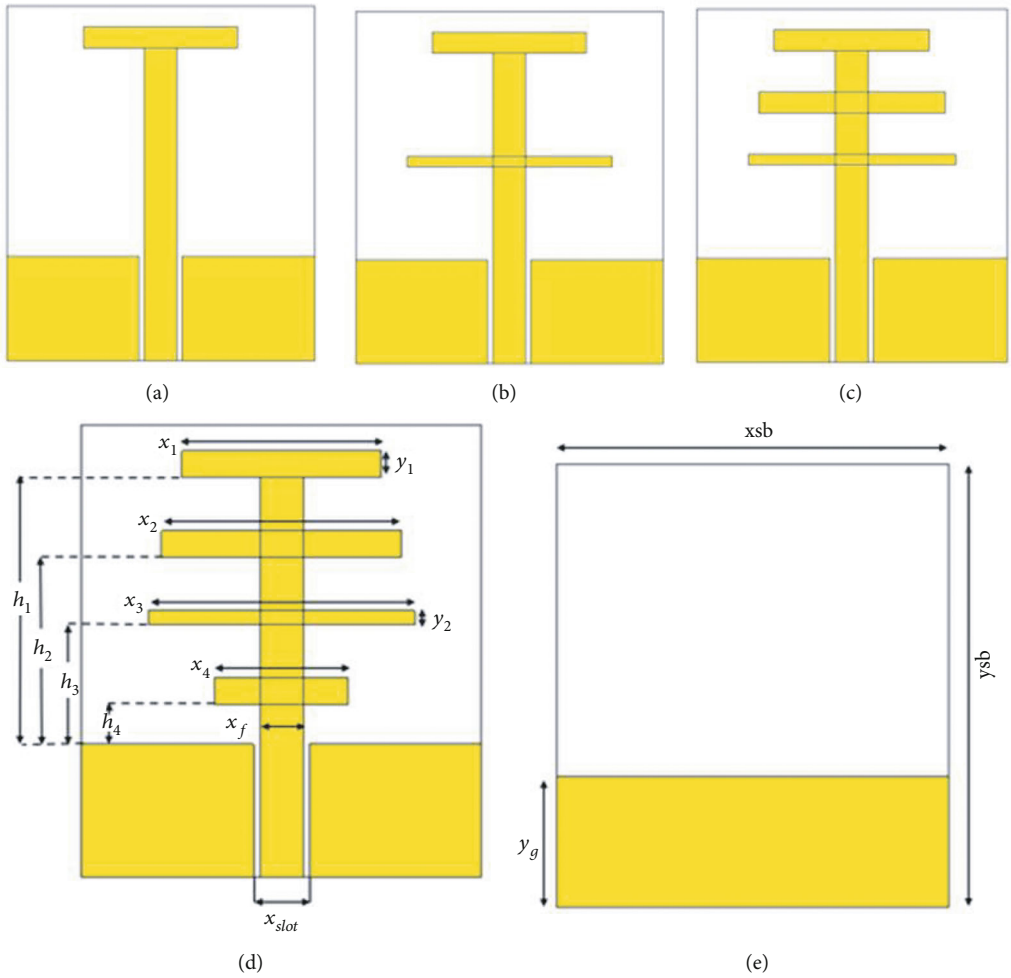

Figure 1: Proposed antenna design process. (a) First step. (b) Second step. (c) Third step. (d) Proposed antenna. (e) The ground plane of the proposed antenna.

Table 1: Dimension for the proposed antenna.

Parameter	Value (mm)	Parameter	Value (mm)	Parameter	Value (mm)
y_{sb}	34	h_1	20	x_{sb}	30
y_g	10	h_2	14	x_1	15
y_1	2	h_3	9	x_2	18
y_2	1	h_4	3	x_3	20
x_f	3.2	x_{slot}	4.2	x_4	10

Non-Ionizing Radiation Protection (ICNIRP) [17]. We have also examined several wearable antennas discussed in [18–20]. It is worth noting that the antenna presented in [20] had a relatively large size of $1.54\lambda \times 0.48\lambda$. Furthermore, although the SAR (specific absorption rate) value was not mentioned in [18], it was found to be suboptimal in [19] at 0.536 W/kg, 0.593 W/kg, and 0.692 W/kg for 3 GHz, 6 GHz, and 10 GHz, respectively.

To overcome these limitations, metamaterial-based EBG layers were used to isolate the body and the antenna

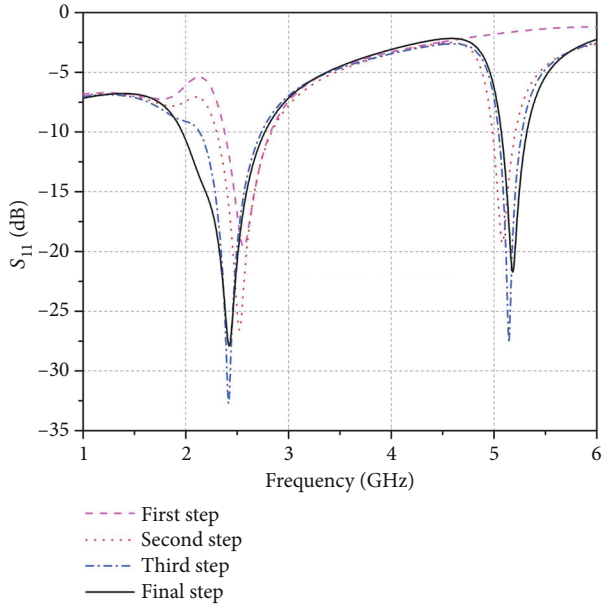

Figure 2: S_{11} based on the evaluation process.

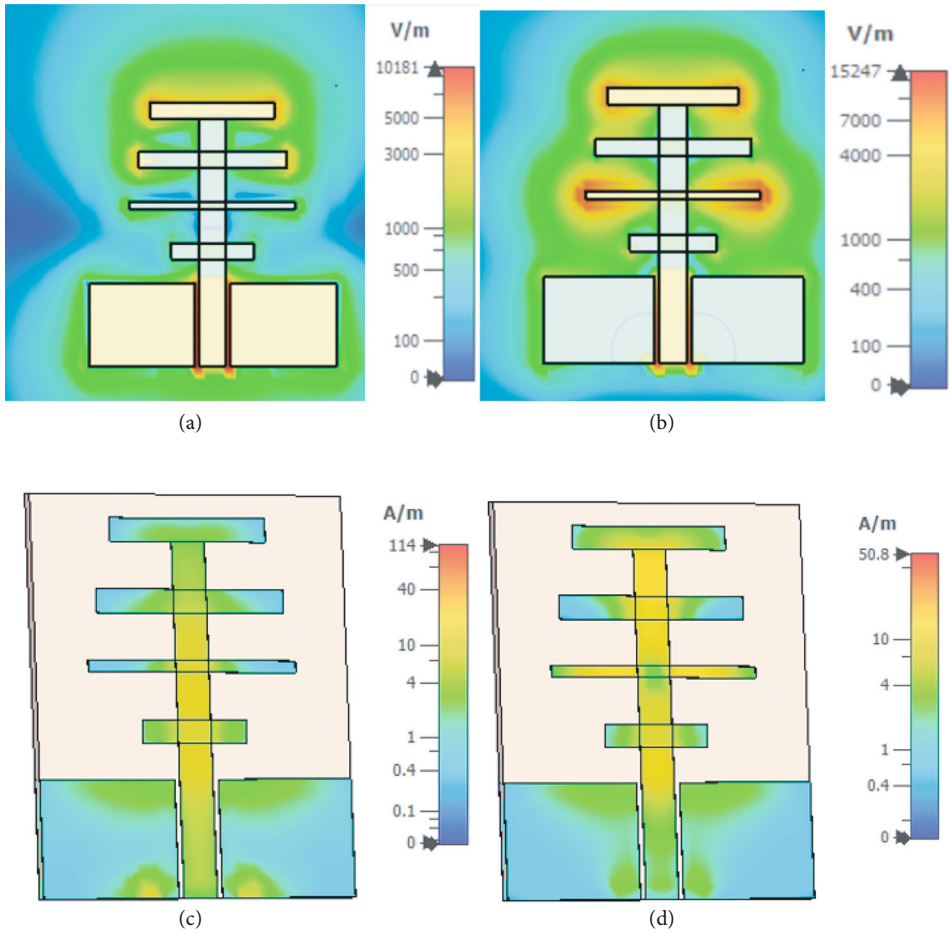

FIGURE 3: Electric field distribution of the proposed antenna at the metal-dielectric interface (a) 2.4 GHz and (b) 5.2 GHz and surface current distribution of the proposed antenna at (c) 2.4 GHz and (d) 5.2 GHz.

in [21], which reduces the SAR values from 2.57 W/kg to 0.68 W/kg. Different structures of the EBG elements were studied such as mushroom structure in [22] and some complex structures in [23], proving the potential function of EBG [24–28] to reduce the interference between the body and the antenna. Unfortunately, the proposed EBG antennas have complex designs and strongly sensitive electromagnetic behavior, which are not suitable for wearable devices.

In this paper, a small-size dual-band T-shaped antenna is proposed using coplanar waveguide (CPW) feed. The application of the rectangular ring-shaped dual-band EBG structure is also investigated, showing the improved wearable antenna SAR. Details of the design principle and the experiment results are shown in the following parts.

2. Antenna and EBG Designs

2.1. Antenna Design. The four-stacked T-shaped antenna fed by CPW is shown in Figure 1. It has four arms with unequal lengths and widths. The antenna parameters are listed as in Table 1. The evaluation process of the design using the T-shaped structure is shown in Figure 1. The first T-arm (first step) in Figure 1(a) responds to the resonance at 2.4 GHz. After adding the second arm as in Figure 1(b), an upper-frequency band appears at 5.2 GHz. Integrating the third and fourth arms corresponding to the third and final steps, respectively, as shown in Figures 1(c) and 1(d), leads to a bandwidth enhancement at the low-frequency resonance at 2.4 GHz (see Figure 2). As in Figure 3, the lower resonant band is determined by the first arm, and its bandwidth (defined at -10 dB of S_{11}) is extended by the third and fourth arms of the antenna. This enhancement is probably due to the coexcitation of resonances at adjacent frequencies, and thus forms a wider operating band. The other resonant band (5.2 GHz) is determined solely by the first and second arms of the antenna. The proposed antenna uses a RT/duroid 5880 substrate with a thickness of 0.8 mm, a relative permittivity of 2.2, and a loss tangent of 0.0009, with a 0.035 mm of the copper layer. This substrate is flexible and resilient, which is suitable for wearable devices. The antenna dimension is listed in Table 1.

To verify the applicability of wearable devices, a simple model (phantom) of a human arm is proposed in this paper. The human arm is modeled using CST and consists of four layers: skin, fat, muscle, and bone, as shown in

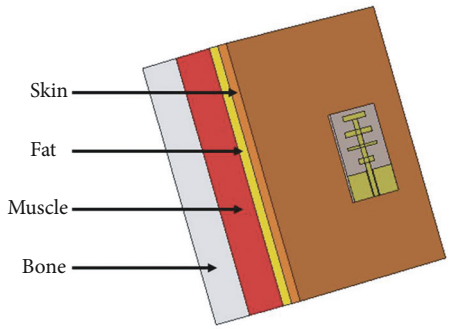

Figure 4: Antenna placed on the human arm modeling.

Table 2: Properties of the human arm.

	Skin	Fat	Muscle	Bone
Dieletric constant	38	5.28	52.79	11.38
Conductivity (S/m)	1.46	0.1	1.73	0.39
Density (kg/m^3)	1100	1100	1060	1850
Thickness (mm)	4	4	16	16

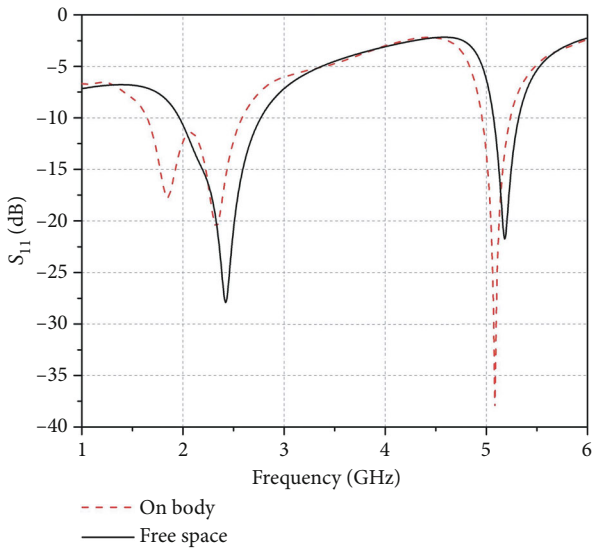

Figure 5: Simulated S_{11} of the monopole antenna in free space and on the body.

Figure 4. The materials and design parameters of the human arm are the same as listed in [29, 30], which have been demonstrated to be suitable for describing the human arm. The intrinsic properties of each layer are summarized in Table 2.

As shown in Figures 5 and 6 when the antenna is placed in free space, it gives two bands, from 1.96 GHz to 2.77 GHz (33.75% bandwidth) and from 5.07 GHz to 5.35 GHz (4.8% bandwidth) for $S_{11} \leq -10$ dB. The antenna peak gain at 2.4 GHz is 1.45 dBi, while that at 5.2 GHz is 1.56 dBi. When the antenna is placed on the body, the operating frequencies were redshifted and split (for the resonance frequency at 2.4 GHz), and their gains decrease dramatically due to the effect of the human arm. Furthermore, the SAR value was extremely high for an input power of 250 mW, as shown in Figure 7. The radiation efficiency also reduces from 84% to 9.2% at 2.4 GHz and from 58.8% to 13.1% at 5.2 GHz.

2.2. EBG Design. To improve the radiation efficiency and reduce the SAR value, the metamaterial-based EBG structure was designed and integrated into the antenna. The proposed EBG structure consists of double-ring rectangles, as shown in Figure 8. The EBG geometrical parameters are shown in Table 3. This EBG operates at both 2.4 GHz and 5.2 GHz. The size of the outer ring, which responds to the single-band resonance at 2.4 GHz, can be adjusted by tuning the parameters x_1, x_2, and x_3. After adding the inner ring, the EBG operates at another frequency, as shown in Figure 9 and the size of this inner ring (x_4, x_5) is tuned to operate at 5.2 GHz. Figure 9 shows that adding the inner ring makes an insignificant change in the 2.4 GHz band. It means tuning either one of two rings has almost no effect on the other one. So, the operating frequencies can be adjusted by tuning the size of each ring independently.

The EBG in free space and on the body can be simplified by an equivalent circuit shown in Figures 8(b) and 8(c). The inner ring is represented by the inductance L_1. The outer loop is featured by the inductance L_2. The central gap gives rise to the capacitance C_1, while the gap between the outer and inner loops responds to the capacitance C_2. The interelement capacitance is denoted by capacitance C_3. The body is characterized by inductance L_4. The gap between the EBG and the body gives rise to C_4. The resonant frequency of each structure can be determined from the total capacitance and inductance of the equivalent circuits.

The EBG has two band gap frequencies, as shown in Figure 9. One of the bands covers the 2.4 GHz peak which has a band gap frequency between 2.06 GHz and 2.73 GHz. Another one covers the 5.2 GHz peak between 4.66 GHz and 5.96 GHz. Figure 9 also shows that the S_{11} value is nearly 0 dB in the range of the band gap frequency, indicating none of the waves in the range of the band gap can be transmitted. The phase of the EBG goes from -90° to +90°, covering a band from 2.08 GHz to 5.24 GHz, as depicted in Figure 10.

3. EBG Antenna Design

When the antenna was placed on the human arm above the EBG, the operating frequencies were shifted away, and the parameters must be reoptimized. The EBG antenna parameters are shown in Table 4.

The wearable antenna using 2×2 EBG unit cells was placed behind the antenna. There is an air gap between the antenna and the EBG structure to avoid impedance mismatching and short circuits. The overall size is $56 \times 56 \times 6.6$ mm^3, as shown in Figure 11.

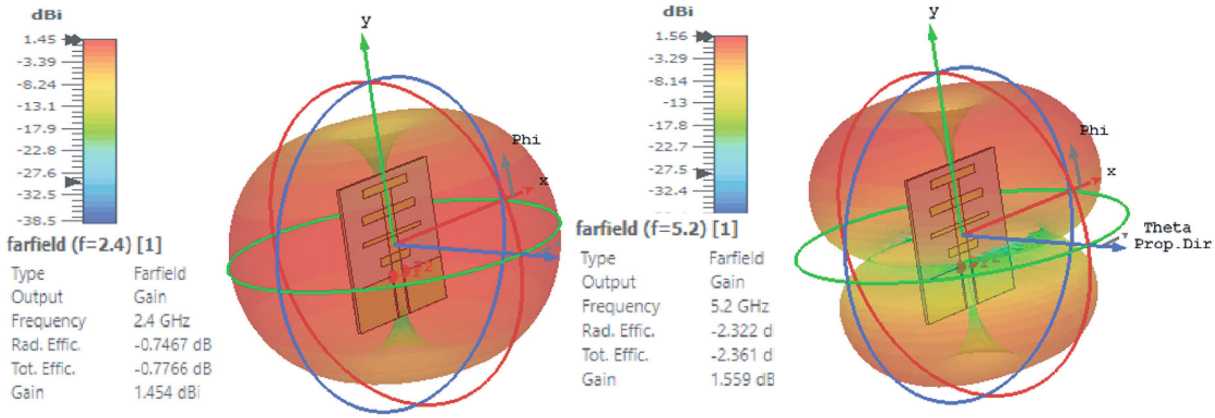

(a)

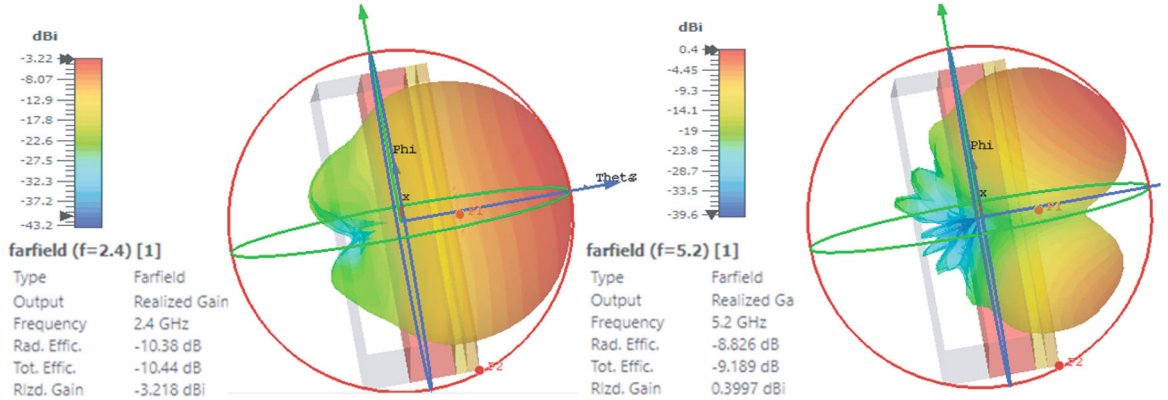

(b)

Figure 6: Simulated radiation patterns of the proposed antenna in (a) free space and (b) on the body.

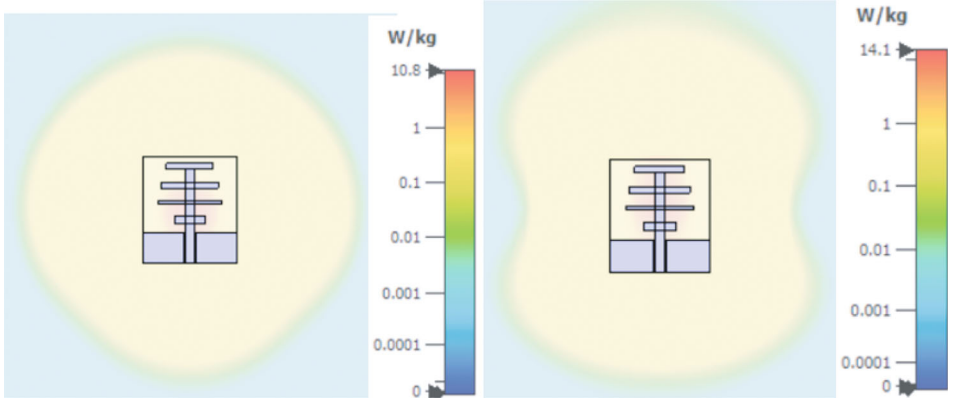

(a) (b)

Figure 7: Simulated SAR of the proposed antenna on body at (a) 2.4 GHz and (b) 5.2 GHz.

To examine the performance of the EBG antenna on the body, its electromagnetic response on the human arm was computed, as illustrated in Figure 11(a). The EBG wearable antenna prototype measurement configuration is presented in Figures 11(b)–11(d). The simulated and measured reflection coefficient results are shown in Figure 12. It was found that the bandwidth of the EBG antenna is smaller than the bare one, from 1.81 GHz to 2.52 GHz (30% bandwidth)

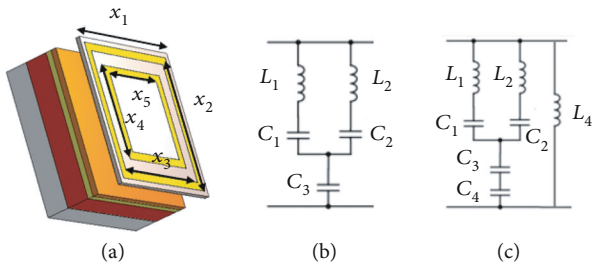

FIGURE 8: (a) An EBG unit cell and its equivalent circuit: (b) in free space and (c) on body.

TABLE 3: Dimension for the proposed EBG unit cell.

Parameter	Value (mm)	Parameter	Value (mm)
x_1	28	x_4	18
x_2	26	x_5	15
x_3	23		

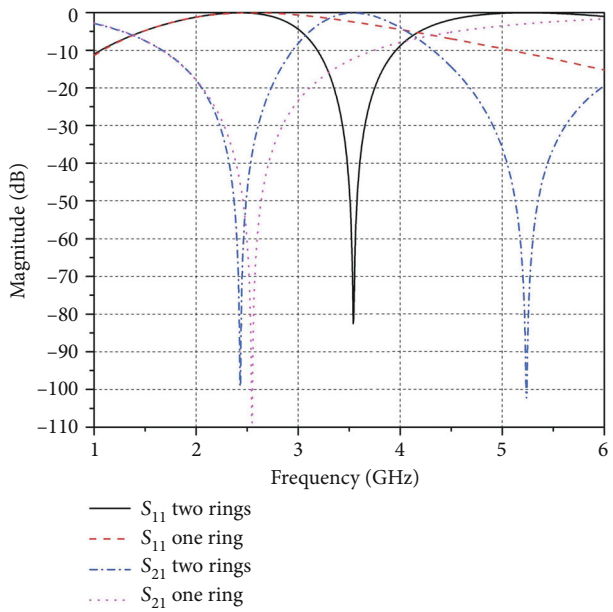

FIGURE 9: Simulated S_{11}, and S_{21} for one and two rings EBG structure.

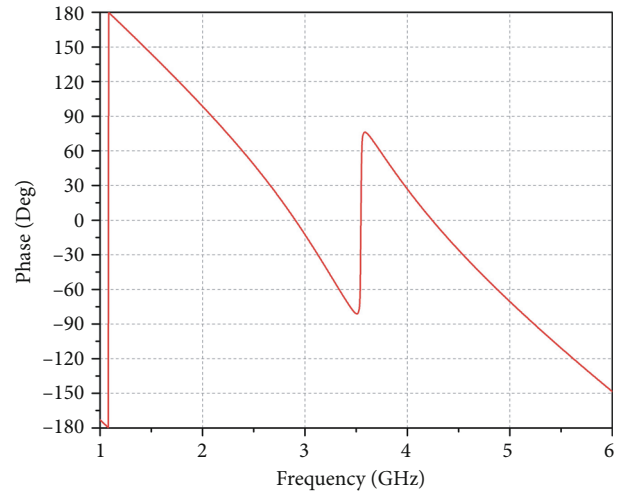

FIGURE 10: Reflection phase of the proposed EBG.

TABLE 4: Dimension for EBG antenna.

Parameter	Value (mm)	Parameter	Value (mm)
y_{sb}	34	x_{sb}	30
y_g	9	x_1	15
y_1	2	x_2	22.5
y_2	2	x_3	8
h_1	20	x_4	10
h_2	14	x_f	2.7
h_3	9	x_{slot}	4.2
h_4	3		

and from 5.14 to 5.3 GHz (3.1% bandwidth), respectively. But the SAR values with the same input power (100 mW) decrease considerably (77.1% at 2.4 GHz and 91.7% at 5.2 GHz), as shown in Figure 13. It is worth mentioning that the gain is impressively improved from 1.56 to 6.25 dBi at 5.2 GHz, as shown in Figure 14.

As shown in Figure 12, the measured bandwidth of the antenna is much smaller than the simulated one, from 2.15 GHz to 2.5 GHz (16.67% bandwidth) and from 5.17 GHz to 5.28 GHz (2.1% bandwidth). Figure 14(c) shows the simulated and measured radiation patterns of the EBG antenna at two frequencies of 2.4 GHz and 5.2 GHz. In general, the results show that the measured radiation patterns coincide with the simulated radiation patterns. There are still some distortions. This might have been caused by the radiation patterns measured at 10°. Besides that, since the antenna was fixed with the EBG by foam, the relative position between the antenna and the EBG may not be as in the simulation. The SMA connector and welding errors also cause some distortions. After adding the EBG structure behind the antenna, the maximum input power increased significantly, as shown in Table 5. The proposed EBG antenna is then connected to the Wi-Fi module to determine the signal-to-noise ratio (SNR) at the frequency band of 2.4 GHz, as shown in Figure 15. The measured SNR of the proposed EBG antenna is 6 dB more than that of the commercial antenna.

Table 6 provides a comparison between the proposed EBG wearable antenna and some related works. As shown in Table 6, the antenna in [14, 24] is smaller than this work, and the antenna in [31] has the largest bandwidth. However, antenna [14] has a very low gain, antenna [24] has a very small bandwidth, and antenna [31] is extremely large. Compared with other reported antennas in Table 6,

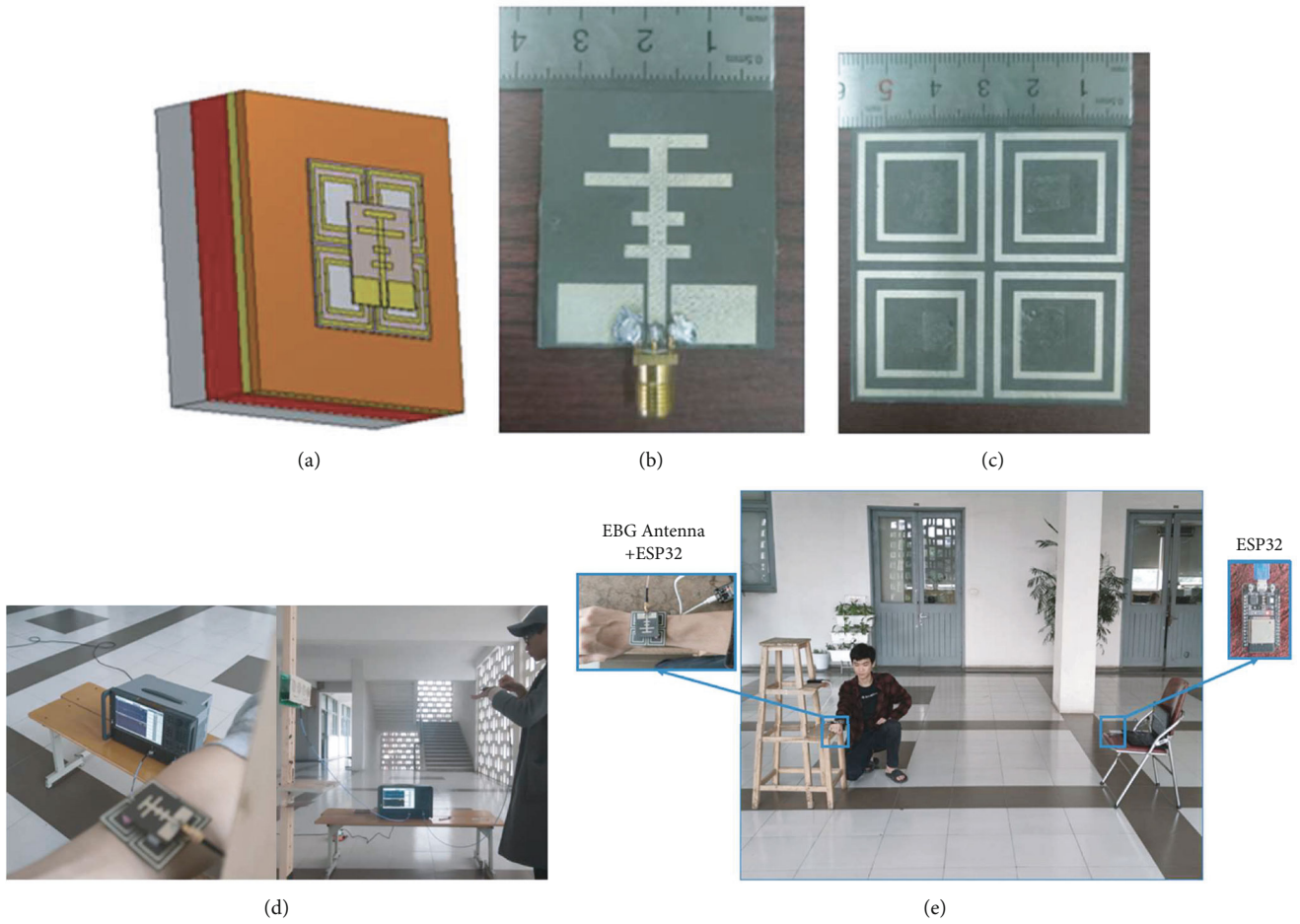

FIGURE 11: (a) The proposed EBG wearable antenna modeling; (b) four-stacked T-shaped antenna prototype; (c) EBG layer prototype; (d) EBG wearable antenna measurement configuration at the laboratory; (e) SNR measurement configuration at the laboratory.

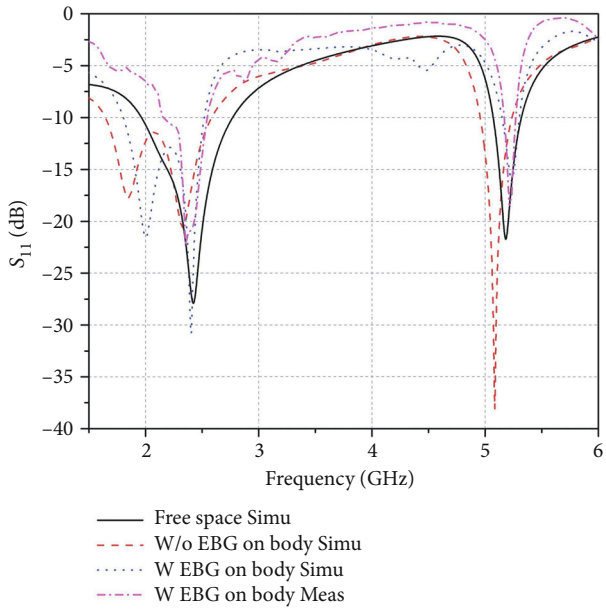

FIGURE 12: Simulated performance of the antenna with and without the EBG structure on the body, in free space, and measured performance of the antenna with the EBG structure.

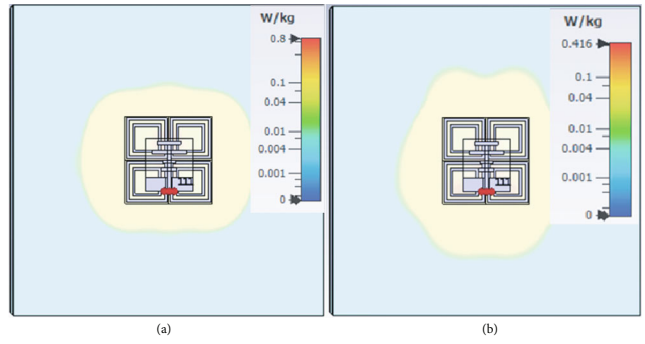

FIGURE 13: Simulated SAR of EBG wearable antenna (a) 2.4 GHz and (b) 5.2 GHz.

the proposed antenna has a wide bandwidth, high gain, acceptable size, and low SAR. In addition, the proposed antenna is validated and tested in a Wi-Fi wearable device as shown in Figure 11(e) showing the improving signal-to-noise (SNR) ratio. The proposed EBG antenna is connected to the Wi-Fi module (ESP32 module) SNR measurement experimentation. We also use an ESP32 module

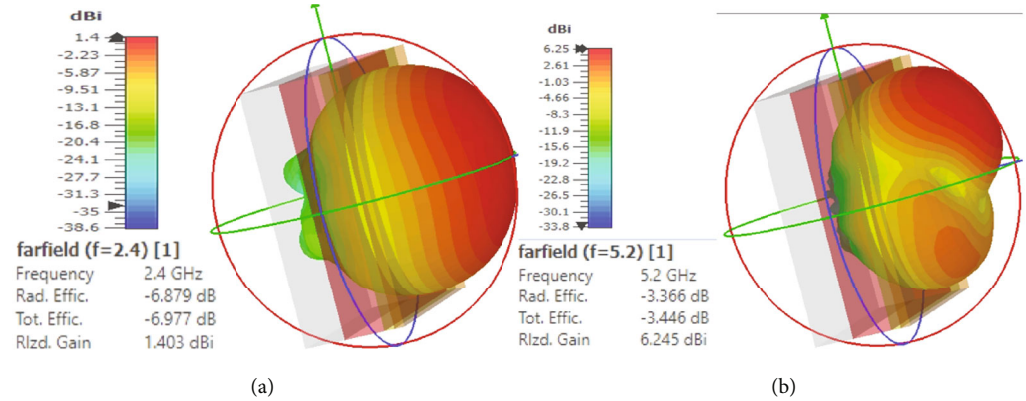

(a) (b)

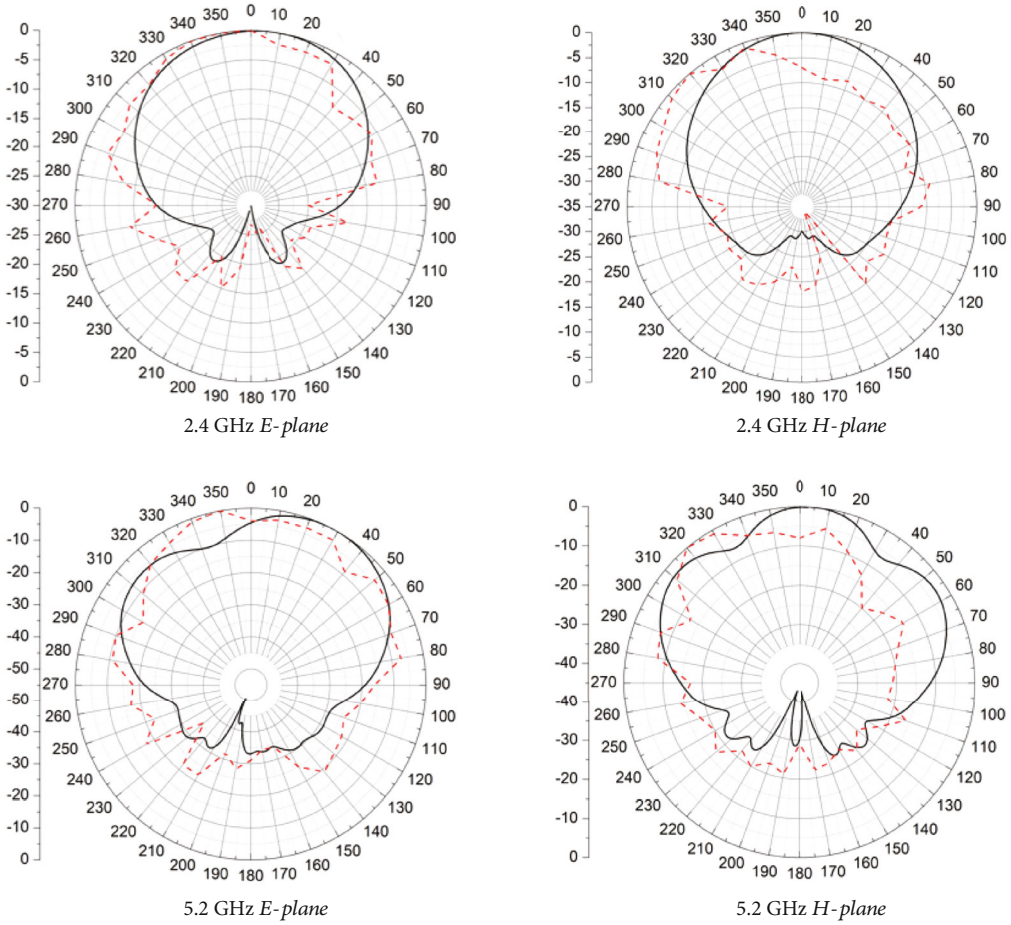

(c)

Figure 14: 3D radiation pattern of wearable EBG antenna at (a) 2.4 GHz and (b) 5.2 GHz. (c) Simulated and measured radiation pattern of the EBG wearable antenna at 2.4 GHz and 5.2 GHz.

Table 5: Maximum input power to meet SAR regulation ICNIRP.

	2.4 GHz	5.2 GHz
Without EBG	90 mW	70 mW
With EBG	310 mW	600 mW

to receive the signal. We determine the Received Signal Strength Indicator (RSSI) and calculate the SNR from the RSSI value and the noise floor. Normally, the noise floor is the sensitivity of the module (about -97 dBm with the ESP32).

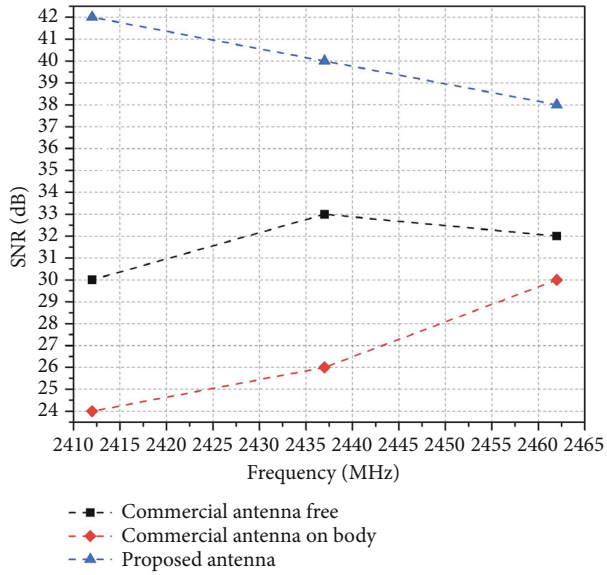

Figure 15: SNR results of the proposed antenna at 2.4 GHz.

Table 6: Comparison of the proposed wearable antenna with related works.

Ref.	Size (mm^2)	Operating frequencies (GHz)	Bandwidth (%)	Gain (dBi)	SAR_10g (W/kg) *P*_input (mW)
[12]	83 × 83	2.4/5.8	4.2	4.5/5.6	0.668/1.51 NA
[14]	50 × 40	2.47/5.42	20/18	1.17/2.26	0.165/0.52 100
[31]	69 × 69	2.45/5.8	3.7/28	7/9.1	0.0452/0.0563 100
[24]	40 × 15	2.4/5.8	4.1/2.5	1.5/4.2	NA
[26]	69 × 69	2.4/3.5/5.8	10/16/7	5.11/6.43/7.41	0.428/0.067/0.035 500
[27]	57 × 57	2.4/3.5/5.8	4.5/5.4/4.5	6.3/7.4/8.7	0.471/0.86/0.1446 100
This paper	56 × 56	2.4/5.2	16.67/2.1	1.4/6.25	0.64/0.333 100

4. Conclusion

In this paper, a wearable T-shaped antenna using 2 × 2 EBG unit cells is designed for onbody wireless communications applications. Without the EBG layer, the basic antenna covers two bands from 1.96 GHz to 2.77 GHz and from 5.07 GHz to 5.35 GHz with a gain of 1.42 dBi at 2.4 GHz and 1.52 dBi at 5.2 GHz in free pace. The measured results show that using an EBG structure reduced the SAR value by 77.1% at 2.4 GHz and 91.7% at 5.2 GHz, and the antenna has a wide bandwidth, a high gain, and an acceptable size. Based on this result, the proposed T-shape antenna over a 2 × 2 EBG array is a strong potential candidate for wearable applications.

Data Availability

Data is included in our manuscript.

Disclosure

Minh Thuy Le present address is the School of Electrical and Electronic Engineering, Hanoi University of Science and Technology, Hanoi, Vietnam.

Conflicts of Interest

The authors declare that they have no conflicts of interest.

Acknowledgments

This research is funded by the Asahi Glass Foundation 2023.

References

[1] K. N. Paracha, S. K. A. Rahim, P. J. Soh, and M. Khalily, "Wearable antennas: a review of materials, structures, and innovative features for autonomous communication and sensing," *IEEE Access*, vol. 7, pp. 56694–56712, 2019.

[2] S. M. Iqbal, I. Mahgoub, E. Du, M. A. Leavitt, and W. Asghar, "Advances in healthcare wearable devices," *NPJ Flexible Electronics*, vol. 5, no. 1, 2021.

[3] L. Jenkins and R. Weerasekera, "Sport-related back injury prevention with a wearable device," *Biosensors and Bioelectronics: X*, vol. 11, article 100202, 2022.

[4] M. Sparaco, L. Lavorgna, R. Conforti, G. Tedeschi, and S. Bonavita, "The role of wearable devices in multiple sclerosis," *Multiple Sclerosis International*, vol. 2018, Article ID 7627643, 7 pages, 2018.

[5] X. Liu, "Intelligent physical training data processing based on wearable devices," *Computational Intelligence and Neuroscience*, vol. 2022, Article ID 1207457, 9 pages, 2022.

[6] S. H. Hwang, J. I. Moon, W. I. Kwak, and S. O. Park, "Printed compact dual band antenna for 2.4 and 5 GHz ISM band applications," *Electronics Letters*, vol. 40, no. 25, p. 1568, 2004.

[7] V. Deepu, K. R. Rohith, J. Manoj et al., "Compact uniplanar antenna for WLAN applications," *Electronics Letters*, vol. 43, no. 2, p. 70, 2007.

[8] G. Srilatha, G. S. Raju, and P. A. S. Dayal, "Compact wearable low-SAR dual band antenna for on body network applications," *International Journal of Communication Systems*, vol. 34, no. 18, 2021.

[9] J. Kulkarni, C.-Y.-D. Sim, and A. Poddar, "Multi band inter connected C-shaped flexible antenna for mobile and fixed wireless communication systems," in *Optical and Wireless Technologies*, M. Tiwari, Y. Ismail, K. Verma, and A. K. Garg, Eds., vol. 892 of Lecture Notes in Electrical Engineering, pp. 329–337, Springer Nature, Singapore, 2023.

[10] J. Kulkarni, A. G. Alharbi, C.-Y.-D. Sim et al., "Dual polarized, multiband four-port decagon shaped flexible MIMO antenna for next generation wireless applications," *IEEE Access*, vol. 10, pp. 128132–128150, 2022.

[11] J. Kulkarni, A. G. Alharbi, C.-Y.-D. Sim, and J. Anguera, "Compact, multiband, flexible decagon ringmonopole antenna for GSM/LTE/5G/WLAN applications," in *2022 16th European conference on antennas and propagation (EuCAP)*, pp. 1–5, Madrid, Spain, 2022.

[12] G. Gao, H. Bin, S. Wang, and C. Yang, "Wearable planar inverted-F antenna with stable characteristic and low specific absorption rate," *Microwave and Optical Technology Letters*, vol. 60, no. 4, pp. 876–882, 2018.

[13] A. Abbosh, H. Al-Rizzo, S. Abushamleh, A. Bihnam, and H. R. Khaleel, "Flexible CPW-IFA antenna for wearable electronic devices," in *2014 IEEE Antennas and Propagation Society International Symposium (APSURSI)*, pp. 1720-1721, Memphis, TN, USA, 2014.

[14] A. Al-Sehemi, A. Al-Ghamdi, N. Dishovsky, N. Atanasov, and G. Atanasova, "Design and performance analysis of dual-band wearable compact low-profile antenna for body-centric wireless communications," *International Journal of Microwave and Wireless Technologies*, vol. 10, no. 10, pp. 1175–1185, 2018.

[15] T. Tuovinen, M. Berg, K. Y. Yazdandoost, and J. Iinatti, "Ultra wideband loop antenna on contact with human body tissues," *IET Microwaves, Antennas & Propagation*, vol. 7, no. 7, pp. 588–596, 2013.

[16] R. Thukral, A. K. Gulshan, and A. S. Arora, "Effects of different radiations of electromagnetic spectrum on human health," in *2020 IEEE International Students' Conference on Electrical, Electronics and Computer Science (SCEECS)*, pp. 1–6, Bhopal, India, 2020.

[17] International Commission on Non-Ionizing Radiation Protection (ICNIRP), "Guidelines for limiting exposure to timevarying electric, magnetic, and electromagnetic fields (up to 300 GHz)," *International Commission on Non-Ionizing Radiation Protection. Health Physics*, vol. 74, no. 4, pp. 494–522, 1998.

[18] A. De, B. Roy, A. Bhattacharya, and A. K. Bhattacharjee, "Bandwidth-enhanced ultra-wide band wearable textile antenna for various WBAN and internet of things (IoT) applications," *Radio Science*, vol. 56, no. 11, 2021.

[19] T. Govindan, S. K. Palaniswamy, M. Kanagasabai et al., "On the design and performance analysis of wristband MIMO/diversity antenna for smart wearable communication applications," *Scientific Reports*, vol. 11, no. 1, article 21917, 2021.

[20] J. Hanna, Y. Tawk, S. Azar et al., "Wearable flexible body matched electromagnetic sensors for personalized non- invasive glucose monitoring," *Scientific Reports*, vol. 12, no. 1, 2022.

[21] M. T. Le, T. P. Tran, and Q. C. Nguyen, "Wearable BLE wireless sensor based on U-shaped EBG monopole antenna," *Journal of Sensors*, vol. 2022, Article ID 8593750, 15 pages, 2022.

[22] H. A. Khan, S. Ullah, M. A. Afridi, and S. Saleem, "Patch antenna using EBG structure for ISM band wearable applications," in *2016 International Conference on Intelligent Systems Engineering (ICISE)*, pp. 157–160, Islamabad, Pakistan, 2016.

[23] Y. Rahmat-Samii, "Electromagnetic band gap (EBG) structures in antenna engineering: from fundamentals to recent advances," in *2008 Asia-Pacific Microwave Conference*, pp. 1-2, Macau, 2008.

[24] K.-L. Wong, H.-J. Chang, C.-Y. Wang, and S.-Y. Wang, "Very-low-profile grounded coplanar waveguide-fed dual-band WLAN slot antenna for on-body antenna application," *IEEE Antennas and Wireless Propagation Letters*, vol. 19, no. 1, pp. 213–217, 2020.

[25] A. Y. Ashyap, S. H. Dahlan, Z. Z. Abidin et al., "An efficient and robust antenna combined with electromagnetic bandgap structure for wearable medical application," *Journal of Physics: Conference Series*, vol. 1529, no. 2, article 022108, 2020.

[26] W. El May, I. Sfar, J. M. Ribero, and L. Osman, "Design of low-profile and safe low SAR tri-band textile EBG-based antenna for IoT applications," *Progress In Electromagnetics Research Letters*, vol. 98, pp. 85–94, 2021.

[27] R. Li, W. Chuan, X. Sun, Y. Zhao, and W. Luo, "An EBG-based triple-band wearable antenna for WBAN applications," *Micromachines*, vol. 13, no. 11, 2022.

[28] T. Govindan, S. K. Palaniswamy, M. Kanagasabai, S. Velan, S. Kumar, and T. R. Rao, "Quad-port electromagnetic band gap (EBG)—backed non-isomorphic multiple-input-multiple-output (MIMO) antenna for wearable applications," *Electronics*, vol. 7, no. 3, article 035020, 2022.

[29] C. Kissi, M. Särestöniemi, T. Kumpuniemi et al., "On-body cavity-backed low-UWB antenna for capsule localization," *International Journal of Wireless Information Networks*, vol. 27, no. 1, pp. 30–44, 2020.

[30] N. Nguyen, N. Ha-Van, and C. Seo, "Midfield wireless power transfer for deep-tissue biomedical implants," *IEEE Antennas and Wireless Propagation Letters*, vol. 19, no. 12, pp. 2270–2274, 2020.

[31] C. Wang, L. Zhang, W. Shenbing, S. Huang, C. Liu, and W. Xianliang, "A dual-band monopole antenna with EBG for wearable wireless body area networks," *Applied Computational Electromagnetics Society*, vol. 36, no. 1, pp. 48–54, 2021.